Retinal Development and The Expression Profiles of Opsins Genes During Larvae Development in *Takifugu Rubripes*

Qi Zhang
Dalian Ocean University
Yumeng Wu
Dalian Ocean University
Weiyuan Li
Dalian Ocean University
Jia Wang
Dalian Ocean University
Huiting Zhou
Dalian Ocean University
Lei Zhang
Dalian Ocean University
Qi Liu
Dalian Ocean University
Liu Ying
Dalian Ocean University
Hongwei Yan (yanhongwei_1985@hotmail.com)
Dalian Ocean University

Research Article

Keywords: Takifugu rubrepes, larvae, retina, vision, opsins genes

Posted Date: January 5th, 2022

DOI: https://doi.org/10.21203/rs.3.rs-1208058/v1

Abstract

Vision is the dominant sensory modality in fish and critical for the survival of fish larvae to detect predators or capture prey. The visual capacity of fish larvae is determined by the structure of the retina and the opsins expressed in the retinal and non-retinal photoreceptors. In this study, the retinal structure and opsin expression patterns during the early development stage of *Takifugu rubripes* larvae were investigated. At around two days after hatching days (dah), the yolk sac of *T. rubripes* disappeared, the mouth was clearly visible and the larvae started swimming and feeding on rotifers. Histological examination showed that at 1 dah, six layers were observed in the retina of *T. rubripes* larva, including the pigment epithelial layer (RPE), photoreceptor layer (PRos/is), outer nuclear layer (ONL), inner nuclear layer (INL), inner plexiform layer (IPL) and ganglion cell layer (GCL). At 2 dah, all eight layers were visible in the retina in *T. rubripes* larva, including RPE, PRos/is, ONL, outer plexiform layer (OPL), INL, IPL, GCL and optic fiber layer (OFL). By measuring the thickness of each layer, opposing developmental trends were found in the thickness of ONL, OPL, INL and IPL, GCL and OFL. The nuclear density of ONL, INL and GCL and ratio of ONL/INL, ONL/GCL and INL/GCL were also measured and the ratio of ONL/GCL ranged from 1.9 at 2 dah to 3.4 at 8 dah and no significant difference was observed between the different developmental stages ($p > 0.05$). No significant difference was observed for the INL/GCL ratio between the different developmental stages, which ranged from 1.2 at 2 dah to 2.0 at 18 dah ($p > 0.05$). The results of quantitative real-time PCR showed that the expression of *rhodopsin*, *LWS*, *SWS2*, *green opsin*, *rod opsin*, *opsin3* and *opsin5* could be detected from 1 dah. These results suggested that the maturation of eye of *T. rubripes* occurred during the period of transition from endogenous to mixed feeding, explaining the need for vision-based survival skills during the early life stages after hatching and for the overall ecology and fitness of *T. rubripes*.

Introduction

In fish, light was shown to be a key environmental factor that influences its growth, survival, development and reproduction throughout various life stages (Boeuf and Le Bail 1999; García-López et al. 2006; Villamizar et al. 2006; Villamizar et al. 2011; Stuart 2013; Bonvini et al. 2016; Chi et al. 2017). In the aquatic habitat, although vision is degraded by the optical properties of water, it is still the dominant sensory modality in teleosts and plays an important role in information transmission in feeding, clustering, reproduction and migration (Guthrie and Muntz 1993; Caves et al. 2018).Lighting regimes that match the larval visual system will increase visual range, decrease search time and ultimately increase growth and survival in artificial breeding setups (Blaxter and Staines 1971; Aksnes and Giske 1993). Although all components of the eye are vital for perceiving a good image, it is the retina that samples the visual environment, transforming light energy as an optical image into electrical energy as a neural image (Evans and Browman 2004; Caves et al. 2018). The mature fish retina has a structure very similar to that of the retinas of other vertebrates, which are composed of a retinal pigment epithelium layer (RPE), outer limiting membrane, photoreceptor layer (PRos/is) excluding the outer nuclear layer (ONL) as the distance from the outer limit of the RPE to the nearest membrane of the ONL, outer plexiform layer (OPL), inner

nuclear layer (INL), inner plexiform layer (IPL), ganglion cell layer (GCL), optic fiber layer (OFL) and the internal limiting membrane. In the retina, the visual information entering the photoreceptors passes through bipolar cells and ganglion cells, then through the optic nerve to the optic lobe (Prasad and Galetta 2001; Jones et al. 2009). The photoreceptor can convert light information into electrical signals. Like all vertebrates, teleosts have two types of photoreceptors, rods and cones, in their retinas and different subtypes of cones recognize different light wavelengths, while rods recognize the intensity of light.

In most vertebrates, light is captured through light-sensitive proteins called opsins, which are expressed in ciliary photoreceptor cells (c-opsins) and encode for G protein-coupled receptors that bind to a light-absorbing, vitamin A-derived nonprotein retinal chromophore (Shichida et al. 1998; Palczewski et al. 2000; Collin et al. 2003; Cortesi et al. 2015; Kasagi et al. 2015). Depending on whether they are directly involved in visual imaging, opsins can be divided into two categories as visual and non-visual opsins (Terakita et al. 2005; Gao et al.2016). Visual opsin proteins are further grouped into five classes spectrally tuned to absorb light at different wavelengths based on both phylogenetic and functional relationships, including medium to long wave-sensitive opsins detecting green to red (*MWS* or *LWS*), short wave-sensitive opsins sensitive to ultraviolet to blue (*SWS1*) and violet to blue (*SWS2*), rhodopsin which is only used in scotopic vision (*RH1*) and rhodopsin-like opsins that detect blue to green (*RH2*) (Hargrave et al. 1983; Yokoyama 1997, 2000; Chinen et al. 2003; Matsumoto et al. 2006; Spady et al. 2006; Carleton et al. 2008; Watson et al. 2011; Escobar-Camacho et al. 2017). Non-visual opsins detect light and perform various non-image forming functions in the retinal and brain neurons in fish, such as regulating biological clocks, activity change, signal transduction and regulation of hormone levels (Jenkins et al. 2003; Nakane et al. 2010; Guido et al. 2020). Fish non-visual opsins include *rod opsin*, *opsin3*, *opsin5*, *tmt-opsin*, *melanopsin*, *pteropsin* and *RH7* (Jenkins et al. 2003; Nakane et al. 2010; Nakane et al. 2014; Beaudry et al. 2017; Guido et al. 2020). In aquaculture, it is important to study the development of retina in fish larvae to understand their physiological activities and ecological adaptability, which allows the light optimization of breeding and growth conditions.

The pufferfish *Takifugu rubripes* of the order *Tetraodontiformes*, family *Tetraodontidae* and genus *Takiugu*, also known as Fugu, is one of the most important marine fish cultured in China, Japan, and Korea because of its delicious taste and high nutritional value. In China, about 70% of the annual product of *T. rubripes* is exported overseas and its domestic consumption is increasing since eating pufferfish became legal in China in 2016 (Katamachi et al. 2015; Kim et al. 2016; Zhang et al. 2019). At present, the scale of breeding of *T. rubripes* is expanding in the coastal area of China. With increasing customer demand, the artificial breeding of *T. rubripes* has become particularly important and optimal lighting regimes for artificial environments are needed based on species and developmental phases (Liu et al. 2019). More important for larval rearing, the lighting conditions need to be matched to the visual system of the target species. Thus, this study investigated the visual system of fugu, including the retinal development and the visual and non-visual protein expression during the early developmental stage of *T. rubripes*.

Materials And Methods

Larval rearing

The eggs of *T. rubripes* were obtained from Dalian Tianzheng Industrial Co., LTD in April 2020 and 2400 larvae were randomly distributed equally into three 300-L cylindrical tanks that were 80 cm high. From 2 days after hatching (dah), fugu larvae were fed with rotifer and artemia to satiation. To remove debris, excess feed, and dead larva and to maintain the quality of the rearing water, the bottom of the tank was cleaned and the water was renewed twice daily. Nitrites and ammonia were measured weekly, while temperature, salinity, pH, and dissolved oxygen were monitored daily. Mean values of nitrites and ammonia were always less than 0.05 mg L^{-1} and 0.2 mg $L^{-1,}$ respectively. Larva were maintained at a temperature of 19.0 to 21.0°C, pH was maintained at 7~8 and the oxygen level was maintained above 8 mg L^{-1}.

Histology and retinal morphometric analyses

At 1, 2, 3, 4, 6, 8, 13, 18, and 26 dah, 20 fugu larva were anesthetized on ice and then fixed in Bouin's fluid for 24 to 28 h either as the whole fish at all stages up to 18 dah or just the heads at 26 dah. According to routine histological techniques, the samples were transferred into 70% ethanol until being prepared for histological analysis. After dehydration in a graded series of alcohol, the samples were embedded in paraffin. Four to six μm sections were cut and stained with hematoxylin-eosin staining (H&E). Sections were observed on a microscope (Leica DM4000 B LED, Leica, Wetzlar, GER) and photographed (Leica DFC450 C, Leica, Wetzlar, GER). Retinal measurements of the sections were made using image analysis software LAS X (Image Pro Plus, v. 4.5, Media Cybernetics, Inc. Rockville, MD, USA) and involved measuring the thickness of each layer RPE, PRos/is, ONL, the ONL, OPL, INL, IPL, GCL, OFL, and the nuclei density of ONL, INL and GCL as the number of ONL nuclei/100 μm, INL nuclei/100 μm, and GCL/100 μm. For each of these parameters, six measurements were performed in the central, dorsal and ventral regions of each retina (n = 9/sampling point). The ratio of thickness of each retinal layer to total thickness (TT), the ratios of number of ONL nuclei to number of INL nuclei, the ratios of number of ONL nuclei to number of GCL nuclei and the ratios of number of INL nuclei to number of GCL nuclei were further calculated.

RNA extraction and Quantitative real-time PCR

At 1, 2, 3, 4, 6, 8, 13, 18, and 26 dah, 20 fugu larva were anesthetized on ice, the whole fish up to 18 dah and the heads only at 26 dah were quickly immersed in ice-cold RNAlater RNA stabilization reagent (Ambion, Austin, TX, USA) and then were immediately transferred to an ultra-low temperature freezer at −80°C until processed. The RNA was extracted using Trizol reagent (Invitrogen, Carlsbad, CA, USA) according to the manufacturer's instructions. The concentration and integrity of the RNA were checked using an Agilent 2100 Bioanalyzer (Agilent Technologies, Santa Clara, CA, USA) and a NanoDrop ND-1000 spectrophotometer (Thermo Scientific, Wilmington, DE, USA).

The specific primers for reference genes and opsins were designed by primer premier 5.0 software (Table 1). Gene expression studies were performed by qPCR. The Applied Biosystems 7900 HT Real-Time PCR System (Applied Biosystems, Foster City, CA, USA) was used with the SYBR FAST qPCR Kit Master Mix (2×) Universal system (KAPA Biosystems, Boston, MA, USA), as recommended by the manufacturer. Briefly, an aliquot of 1 μg of RNA pretreated with DNase I (37°C, 30 min) was used as a template for cDNA synthesis with random hexamers according to the user information for 1st Strand cDNA Synthesis Kit (Takara Bio Inc., Otsu, Japan). Amplification was conducted with an initial denaturation at 95°C for 5 min, followed by 40 cycles of amplification at 95°C for 3 s and 60°C for 20 s. Melting curves were plotted to ensure that a single polymerase chain reaction (PCR) product amplification was obtained for each pair of primers. The stability of *T. rubripes* was verified using Normfinder (v 0.953) (17-20) and the results showed that *β-actin* was comparatively more stable in the present study. The qPCRs were conducted in triplicates and the relative gene expression was calculated using $2^{-\Delta\Delta CT}$, where ΔCT = cycle threshold (CT) of the target gene minus the CT of *β-actin*, and ΔΔCT = ΔCT of any sample minus the calibrator sample method.

Table 1
Primers used for qPCR in the present study

Gene name	Primer	Sequence of primer	Product length(bp)
Rhodopsin	Forward	GAACTACGTCCTGCTCAACCTG	148
	Reverse	CCCTCCTAAAGTGGCAAAGAAT	
LWS	Forward	CAATGTGCGTCTTTGAGGGT	231
	Reverse	TCTTCAGTCCATGAGGCCAG	
SWS2	Forward	GGGACACCATTTGATCTGAGAC	106
	Reverse	AGCGGAACTGTTTATTGAGGAC	
green opsin	Forward	CCGCTGTCAATGGCTACTTC	190
	Reverse	GTGAAAGCGACTCCAACTGC	
Rod opsin	Forward	GGGGAGAATCACGCAATCA	195
	Reverse	GAGGAAGTGGCAGACGAACA	
Opsin3	Forward	CAGCGTCCCAGTCTTTCAGT	190
	Reverse	TCAGGCGTCTTCTTCCATTT	
Opsin5	Forward	GACGGTTGAGGAAGGGCTAT	181
	Reverse	GCTGGCTGTGCTGTCAAGA	
beta-actin	Forward	AACCAAATGCCCAACAACTTC	213
	Reverse	GATCCCCAGATGCAACAGAAC	

Statistical analysis

One-way ANOVA followed by the Tukey's test (IBM SPSS statistics version 22.0, IBM, Chicago, IL, USA) was performed to examine the statistical significance of all data. A p value of < 0.05 was considered significant.

Results

Morphological observations of larvae in various stages

Hatching occurred over two days and hatching time was not synchronous (Fig. 1). At 1 dah, the brain appeared very large in lateral views and the larvae displayed the characteristic roundish body shape of a puffer fish. The larvae still had plenty of yolk and oil droplets within the yolk sac. The pigmentation of the larvae by both erythrophores (red), melanophores (black) and xanthophores (yellow) spread and covered the yolk sac and eye pigmentation emerged. The tail of the larvae was completely pigment free and there was a sharp margin where the pigmentation ended in front of the tail. Most of the larvae had the mouth located midventral between the eyes and punctate melanin on the yolk sac. At 2 dah, the tail of the larva was still completely pigment free, the mouth was clearly visible and the anterior tip of the mouth began protruding beyond the eyes. The larva seemed to have used up all its maternally supplied nutrients. Reflective iridophores became prominent in the eyes and the abdominal pigment gradually accumulated into stellate in most of the larvae. Most of the larvae started swimming, and feeding on rotifers. Pigmentation was more intense and extensive than was observed at 1 dah and especially increased at the dorsal region of the larva. At 3 dah, the dorsal fin bud was clearly observed. At 8 dah, the teeth of larvae were formed, the air sac appeared and they began to attack each other. The pectoral fins were well developed and the caudal fins were clearly visible. From 18 dah, filamentous rays were observed on the caudal fin and the melanophores began to appear in the tail. The fin rays were observed on caudal fins at 26 dah. Larvae were also very similar to adult *T. rubripes* at that point (Fig. 1).

Observation of retinal microstructures at various stages

At 1 dah, six layers were observed in the retina in *T. rubripes* larva, including RPE, PRos/is, ONL, INL, IPL and GCL. At 2 dah, all eight layers were observed in the retina in *T. rubripes* larva, including RPE, PRos/is, ONL, OPL, INL, IPL, GCL and OFL (Fig. 2). The thickness of each layer was shown in Table 2, where the thickness of the RPE increased gradually from 9.3 ± 0.8 μm at 1 dah to a maximum value at 26 dah of 20.0 ±1.5 μm. At 1, 2, 3, 4, 6, and 8 dah, no significant differences were observed in the thickness of the RPE ($p > 0.05$). The thickness of the PRos/is also significantly increased from 3.6 μm at 13 dah (p □ 0.05), reaching a maximum value of 10 μm at 26 dah. No significant difference was observed at 13, 18 and 26 dah ($p > 0.05$). The thickness of the ONL slightly increased initially, reached a maximum value 7.9 μm at 2 dah, then slightly decreased, reaching a minimum value of 4.5 μm at 13 dah. Subsequently, the value increased from 18 dah. The OPL was detected from 2 dah, with its thickness increasing gradually from 2.2 ± 0.3 μm at 2 dah, to a maximum of 5.2 μm at 26 dah. At 1 dah, the thickness of INL was 30.1 ± 1.2

μm, then the value decreased from 3 dah, reaching a minimum value of 18.9 μm at 8 dah, but significantly increasing again between 13 and 26 dah. The thickness of IPL increased gradually from 1 dah, reaching a maximum value of 28.6 μm at 26 dah. The thickness of GCL initially increased slightly to 30.7 μm at 2 dah, then decreased gradually to a minimum value of 13.9 μm at 18 dah. The OFL was observed from 2 dah and then gradually increased to a maximum of 9.4 μm at 26 dah. The total thickness of retina also gradually increased from 78.4 ± 4.1 μm at 1 dah, reaching a maximum value of 120.8 μm at 26 dah.

Table 2
Relative changes in the thickness of retinal layers (μm) in each growth stage of *Takifugu rubripes*

	RPE	PRos/is	ONL	OPL	INL	IPL	GCL	OFL	TT
1 dah (n = 9)	9.3 ± 0.8^{ab}	3.6 ± 0.0^{a}	6.2 ± 0.2^{ab}	—	30.1 ± 1.2^{d}	3.8 ± 0.2^{a}	29.9 ± 0.4^{de}	—	78.4 ± 4.1^{a}
2 dah (n = 9)	8.1 ± 0.4^{a}	4.5 ± 0.1^{a}	7.9 ± 0.7^{b}	2.2 ± 0.3^{b}	29.8 ± 0.7^{d}	10.1 ± 2.5^{ab}	30.7 ± 0.4^{e}	3.2 ± 0.3^{b}	97.1 ± 5.4^{b}
3 dah (n = 9)	11.3 ± 0.4^{abc}	5.0 ± 0.2^{ab}	6.3 ± 0.1^{ab}	3.2 ± 0.4^{bc}	24.8 ± 1.0^{bc}	19.4 ± 1.5^{cde}	25.0 ± 1.6^{cd}	4.9 ± 1.1^{b}	100.7 ± 2.0^{b}
4 dah (n = 9)	11.4 ± 0.5^{abc}	5.7 ± 0.3^{abc}	5.1 ± 0.3^{a}	2.9 ± 0.2^{bc}	20.6 ± 0.5^{ab}	16.0 ± 0.4^{bc}	20.5 ± 1.3^{bc}	4.9 ± 1.1^{b}	90.1 ± 3.5^{ab}
6 dah (n = 9)	12.4 ± 0.5^{bc}	5.9 ± 0.5^{abc}	4.6 ± 0.4^{a}	2.8 ± 0.2^{bc}	19.5 ± 0.8^{a}	17.3 ± 1.9^{cd}	16.2 ± 0.6^{ab}	4.4 ± 0.4^{b}	86.5 ± 0.4^{ab}
8 dah (n = 9)	11.5 ± 0.4^{abc}	4.4 ± 0.3^{a}	4.8 ± 0.5^{a}	3.2 ± 0.6^{bc}	18.9 ± 0.3^{a}	22.8 ± 0.7^{cdef}	17.9 ± 1.9^{ab}	7.1 ± 0.9^{bc}	86.1 ± 6.1^{ab}
13 dah (n = 9)	12.6 ± 0.7^{bc}	7.4 ± 1.0^{bcd}	4.5 ± 0.4^{a}	3.0 ± 0.1^{bc}	19.1 ± 0.5^{a}	23.1 ± 1.4^{def}	15.0 ± 0.6^{a}	5.3 ± 0.8^{bc}	90.4 ± 2.2^{ab}
18 dah (n = 9)	14.4 ± 0.9^{c}	8.3 ± 0.8^{cd}	5.5 ± 0.4^{ab}	4.2 ± 0.4^{cd}	20.0 ± 0.7^{a}	25.9 ± 0.9^{ef}	13.9 ± 0.6^{a}	5.0 ± 0.3^{b}	97.5 ± 3.6^{b}
26 dah (n = 9)	20.0 ± 1.5^{d}	10.0 ± 0.7^{d}	7.9 ± 1.2^{b}	5.2 ± 0.3^{d}	25.9 ± 1.7^{cd}	28.6 ± 1.2^{f}	14.4 ± 1.1^{a}	9.4 ± 1.2^{c}	120.8 ± 2.2^{c}

The ratio of each layer thickness relative to the total thickness was also calculated in Fig. 3. The RPE/TT and PRos/is/TT gradually increased from 2 dah. The value of ONL/TT initially decreased from 2 dah and then increased from 18 dah. The value of OPL/TT increased from 2 dah and reached a value of 5% at 18 dah. The value of INL/TT decreased from 0.38 at 1 dah and reached a value of 20% at 18 dah. Like the value of OPL/TT, the value of IPL/TT increased at 1 dah (8%). Like INL/TT, the value of GCL/TT increased from 1 dah, with a minimum value of 12% at 26 dah. The value of OFL/TT increased from 3% at 2 dah and reached a maximum value of 8% at 26 dah. The nuclear density of ONL, INL and GCL, and the ratios of ONL/INL, ONL/GCL and INL/GCL are shown in Table 3. The nuclear density of ONL increased gradually from 2 dah, attained a maximum value of 213460 at 13 dah and then decreased

slightly subsequently. The nuclear density of INL and GCL also increased gradually from 1 dah. The ONL/INL ratio increased to 1.7 ± 0.1 from 1 dah and then decreased from 13 dah when it had reached 2.3 ± 0.1. The ratio of ONL/GCL ranged from 1.9 at 2 dah to 3.4 at 8 dah and no significant difference was observed among the different sampling points. Like the ratio of ONL/GCL, no significant difference was observed among the different sampling points for the INL/GCL ratio, which ranged from 1.2 at 2 dah to 2.0 at 18 dah.

Table 3

Nuclear density (mm^{-2}/100 μm) of ONL, INL and GCL, and ratio of ONL/INL, ONL/GCL and INL/GCL at different sampling point

	ONL	INL	GCL	ONL/INL	ONL/GCL	INL/GCL
1 dah (n = 9)	89958 ± 7376^{a}	54235 ± 1320^{a}	36448 ± 612^{a}	1.7 ± 0.1^{ab}	2.5 ± 0.2^{a}	1.5± 0.0^{ab}
2 dah (n = 9)	89506 ± 15753^{a}	55999 ± 3906^{ab}	45706 ± 1666^{ab}	1.6 ± 0.2^{ab}	1.9 ± 0.3^{a}	1.2 ± 0.1^{a}
3 dah (n = 9)	160573 ± 10284^{ab}	76957 ± 2899^{abc}	59826 ± 3702^{bc}	2.1 ± 0.1^{ab}	2.7 ± 0.1^{a}	1.3 ± 0.1^{a}
4 dah (n = 9)	200462 ± 16766^{b}	81877 ± 3030^{abc}	55366 ± 3317^{abc}	2.5 ± 0.2^{b}	3.7 ± 0.4^{a}	1.5± 0.0^{ab}
6 dah (n = 9)	206584 ± 24091^{b}	85075 ± 2814^{bcd}	70805 ± 2279^{c}	2.4 ± 0.2^{b}	2.9 ± 0.4^{a}	1.2 ± 0.1^{a}
8 dah (n = 9)	205943 ± 27561^{b}	102339 ± 4509^{cd}	62998 ± 6039^{bc}	2.0 ± 0.3^{ab}	3.4 ± 0.7^{a}	1.7 ± 0.1^{ab}
13 dah (n = 9)	213460 ± 18285^{b}	92423 ± 3468^{cd}	71367 ± 4897^{c}	2.3 ± 0.3^{b}	3.0 ± 0.2^{a}	1.3 ± 0.1^{a}
18 dah (n = 9)	189536 ± 20458^{b}	144007 ± 8867^{e}	71381 ± 3927^{c}	1.3 ± 0.2^{a}	2.7 ± 0.4^{a}	2.0 ± 0.1^{b}
26 dah (n = 9)	144339 ± 7996^{ab}	114206 ± 13507de	67727 ± 6526^{c}	1.3 ± 0.1^{a}	2.2 ± 0.1^{a}	1.7 ± 0.2^{ab}

Expression of retinal related genes

The results of qPCR showed that the expression of *rhodopsin*, *LWS*, *SWS2*, *green opsin*, *rod opsin*, *opsin3* and *opsin5* could be detected from 1 dah, as seen in Fig. 4. No significant difference was observed in the expression of *rhodopsin* from 1 to 4 dah, then the expression increased till 13 dah and then subsequently decreased. It again increased from 18 dah to a maximum at 26 dah (p < 0.05). The gene expression of *LWS* increased gradually from 1 dah and reached at the maximum value at 26 dah. The gene expression of *SWS2* initially increased from 1 dah, decreased from 4 and finally increased from 18 dah. The gene expression of *green opsin* initially increased from 1 dah and then decreased from 8 dah. The expression

of *rod opsin* gradually increased from 1 dah, reached at the maximum value at 26 dah and no significant difference was observed from 1 to 8 dah ($p > 0.05$). No significant difference was observed in the expression of *opsin3* from 1 to 13 dah ($p > 0.05$), with the maximum at 18 dah, which was significantly higher than other sampling points ($p \leq 0.05$) and then decreased from 18 to 26 dah. The gene expression of *Opsin5* increased from two dah and then decreased at 8 dah, and then increased from 13 dah again.

Discussion

Before first feeding, the yolk is utilized for embryo development in most marine fish. As yolk reserves are gradually exhausted, larvae undergo the difficult transition from endogenous to mixed feeding period to obtain energy and required nutrients to support growth and development (Ma et al. 2010; Yúfera et al. 2014). Changes in the behavior of marine fish larvae are closely related to the development of the sensory organs, especially the visual system, which is crucial for feeding and predator defense in larval survival (Lim and Mukai 2014). It is very important for larvae to complete the differentiation of retinal functional cells and mouth-opening before the yolk sac is depleted because food intake requires coordination of food searching, detection, attract, capture and ingestion (Rønnestad et al. 2013, Lim and Mukai 2014, Hu et al. 2018). In this study, the yolk sac of *T. rubripes* disappeared and the larvae were mouth opening and feeding on rotifers at 2 dah. Histological observation showed that all the ten retinal layers were visible in *T. rubripes* from 2 dah, indicating that the well-developed visual system provided the necessary conditions for larval feeding. This result is consistent with other reports in teleosts, such as *Danio rerio*, where the iridophores are scattered over the retina, where the iris will develop and mouth is opening and feeding at 2 dah (Kimmel et al. 1995). In *Epinephelus akaara* larvae, yolk absorption was complete at 3 dah, and the mouth had opened at 4 dah. Hatched larvae had ONL, INL, and GCL starting from 2 to 3 dah, the retina was differentiated into PRE, PRos/is, ONL, OPL, INL, IPL, GCL and the choroid membrane was pigmented at 4 dah (Kim et al. 2013; Kim et al. 2019). In *Engraulis anchoita*, the eyes were pigmented and the GCL and the PR were visible in the retina, towards the end of yolk sac stage, when the larvae were 4 mm in length. This stage of acquisition of functionality coincided with the absorption of yolk and the beginning of exogenous feeding (Miranda et al. 2020). In *Sparus aurata*, the maturation of eye also occurred at 3 to 4 dah and it underwent profound anatomical and physiological alterations, such as the opening of the mouth and anus, the resorption of the yolk sac and functional differentiation of the alimentary canal, liver and pancreas (Parry et al. 2005; Yúfera et al. 2014; Pavón-Muñoz et al. 2016). In contrast, for precocial fish species, such as *Hippocampus reidi*, *Iago omanensis* (Triakidae), *Chiloscyllium punctatum* and *Scyliorhinus canicular*, the retina was fully developed prior to birth (Fishelson and Baranes 1999; Sánchez-Farías and Candal et al. 2005, 2008; Ferreiro-Galve et al. 2008, 2010a, b, 2012; Harahush et al. 2009; Bejarano-Escobar et al. 2012, 2013; Sánchez-Farías and Candal 2015, 2016; Novelli et al. 2015; Álvarez-Hernán et al. 2019), so the degree of maturation at hatching in the retina of fishes is different in altricial and precocial fish species. And, for the most primitive vertebrates, such as sea lamprey *Petromyzon marinus*, begin retinal development during embryogenesis but do not complete differentiation until metamorphosis, occurring well after birth at five or more years of age (De Miguel and Anadón 1987; Rodicio et al. 1995; Harahush et al. 2009).

The RPE layer and the PRos/is layer can be observed early from 1 dah in *T. rubripes*. Although the teleost eye is very similar to the mammalian eye, it is characterized by several unique structures, such as teleost eyes lake eyelids except for the nictitating membranes of certain sharks and most teleost cannot alter the size of their pupil (Kusmic and Gualtieri 2000; Reckel et al. 2002), so the fish retina is more susceptible to potential light-induced damage as they are continuously exposed to intense light. Consequently, alternative protective strategies have developed to cope with high light intensities, including migration of melanin granules and photoreceptor mobility. Acting as an anti-oxidant adjacent to the outer segments of photoreceptor cells, ocular melanin protects the retina against light-induced cell toxicity (Sanyal and Zeilmaker 1988), by migrating in an apical direction in response to light within processes of the RPE and enshroud photoreceptors compared to higher vertebrate (Allen and Hallows 1997). These photoreceptors can move into or out of the deep recesses of the RPE, so the RPE layer develops earlier in *T. rubripes*, which may be critical to protects the retina against light-induced cell toxicity. The results are consistent with some previous studies in other teleost. For example, in *Acanthopagrus latus, Mugil cephalus* and *Alosa sapidissima*, before the retina developed, a thin layer of RPE containing a few melanin particles was clearly observed at the edge of the retina (He et al. 1985; Xu et al. 1988, Gao et al. 2016). In this study, opposing developmental trends were found in the thickness of ONL and OPL, INL and IPL, GCL and OFL in *T. takifugu*. In teleost, the ONL is composed of the cell bodies of the cones and rods. The OPL contains the processes and synaptic terminals of rods, cones, horizontal cells and bipolar cells. The nuclei of the bipolar cells, amacrine cells, horizontal cells and Müller cells are found in the INL and the IPL consists of the connections between bipolar, amacrine and ganglion cells. The nuclei of ganglion cells form the GCL and the OFL contains the axons of ganglion cells as they collect to form the optic nerve (Fernald 1990; Kolb 2011; Ferreiro-Galve et al. 2008, 2010a, b, 2012; Bejarano-Escobar et al. 2014; Musilova et al. 2019). Cell body and synaptic differentiation becomes more obvious, resulting in a continuous decrease in the thickness of ONL and an increasing thickness of OPL (Ali and Anctil 1977; Kolb 2011). Similarly, with the extension of axons and the continuous branching of dendrites, the thickness of INL decreases and the thickness of IPL increases (Ali and Anctil 1977; Kolb 2011). With the extension of axons and dendrites, the thickness of GCL decreases and the thickness of OFL increases (Ali and Anctil 1977; Kolb 2011). The results obtained in the present study reflect the differentiation process of the retina during the early developmental stage of *T. rubripes*. The emergence of the plexiform layers occurs almost simultaneously, as have been described in other fast-developing teleost (Parry et al. 2005; Bejarano-Escobar et al. 2012, 2013; Pavón-Muñoz et al. 2016). In contrast, studies conducted in slow-developing species such as elasmobranchs and *Sparus trutta* have shown that the IPL evolves earlier than the OPL (Ferreiro-Galve et al. 2008, 2010a, b, 2012; Harahush et al. 2009; Bejarano-Escobar et al. 2012; Sánchez-Farías and Candal et al. 2005, 2008).

In a previous study, the ONL/INL ratio was used to estimate the degree of spatial summation of visual information at the first synapse in the retina and compared to crepuscular at 1.4 to 1.7 or nocturnal 2.7 to 3.5 foraging species, diurnal feeding fishes were shown to have a lower summation ratio of 0.5 to 1.4 (Munz and McFarland 1973; Schieber et al. 2012). In nocturnal fishes, the higher ratio increases visual sensitivity by pooling the signals from many photoreceptors, at the expense of spatial resolving power,

which reflects the adaptation to dim conditions (Munz and McFarland 1973). In the present study, the ONL/INL ratio of *T. rubripes* was 1.3 to 2.5 during the early developmental stage, suggesting that the fugu larvae have higher visual sensitivity. As reported previously, the female *T. rubripes* lays demersal, adhesive eggs in coastal waters at a depth of 10 to 50 m during spring, and juveniles remain in nursery ground areas near the main spawning grounds from spring to summer, and then enter wider areas (Katamachi et al. 2015; Kim et al. 2016; Zhang et al. 2019). The higher ratio of the ONL/INL in *T. rubripes* reflects an adaptation to their surrounding light conditions. However, Schieber et al. (2012) examined the retinal anatomy of four elasmobranch species with differing ecologies, including Port Jackson shark *Heterodontus portusjacksoni*, the bull shark *Carcharhinus leucas*, pink whipray *Himantura fai*, and the epaulette shark *Hemiscyllium ocellatum* and found that the ONL:INL ratio may be a less robust indicator of diel activity patterns in elasmobranchs. The ratio of the nucleus number of the ONL layer to the GCL layer reflects the degree of retina network convergence (Xu et al. 1998), and this reflects the degree of visual sensitivity and light sensitivity of fish (Ma et al. 2010). Higher visual sensitivity helps them to distinguish small aquatic organisms such as zooplankton in motion providing the possibility of successful predation (Ma et al. 2010). In this study, no significant difference was observed among the different sampling points, which ranged from 1.9 to 3.7, which suggested that *T. rubripes* may acquire high visual sensitivity before the larvae open their mouths.

The vertebrate visual opsin genes are expressed in the retina and are responsible for facilitating visual perception. The expression of visual genes like *rhodopsin*, *LWS*, *SWS2* and *green opsin*, and non-visual genes like *opsin3* and *opsin5* in *T. rubripes* were detected early from 1 dah, suggesting the fugu larvae may be able to detect different wavelength spectra, especially detecting the short wavelength light could increase the contrast of prey against the water background (Hargrave et al. 1983; Loew et al. 1993; Browman et al. 1994). A similar pattern was also observed in most fish species, including *Clupea pallasi*, (Sandy and Blaxter 1980), *Pseudopleuronectes americanus* (Mader and Cameron 2004), and *Oncorhynchus nerka* (Flamarique and Hawryshyn 1996). Previous studies have shown that the *SWS*, including ultraviolet/violet or short-wavelength sensitive type 1 cone opsins (*SWS1*; approx. 360–430 nm) and blue or short-wavelength sensitive type 2 cone opsins (*SWS2*; approx. 430– 460 nm) (Jacobs et al. 1996; Van et al. 2006). The light-sensitive pigments of *SWS1* can absorb the maximum spectral range of incident light within the spectrum of ultraviolet, which plays a significant role in foraging, communication and mate selection. The *SWS1* genes have been isolated from a surprisingly wide range of vertebrates, including lampreys, teleosts, amphibians, reptiles, birds, and mammals (Van et al.2006). However, previous studies have shown that no sequence related to the *SWS1* gene was found in the transcriptome of *T. rubripes* eyeball tissue, indicating that this gene was lost in a common *Tetraodontiform* ancestor after the Percomorph radiation (Neafsey et al. 2005). Fish possess *SWS2* opsin, which is absent in most mammals, including humans, except for a few marsupials and monotreme species. The expression levels of the fish non-vision genes, *rod opsin*, *opsin3* and *opsin5* were measured. *Rod opsin* can restore visual functions in retinal degeneration and mutations in rod opsin cause neurodegenerative blindness retinitis pigmentosa (Athanasiou et al. 2012; Rennison et al. 2012). *Rod opsin*-treated mice can detect visual stimuli in a dimly lit room, including a flicker at a range of frequencies (up to 10Hz), differences in

luminance commonly encountered in visual scenes (Jasmina et al. 2015). In this study, *rod opsin* was expressed from 1 dah in *T. rubripes* and gradually increased, which suggested that the protection function of the retina in *T. rubripes* was gradually increasing. The *opsin3*, also known as cerebral opsin or panopsin, is a protein encoded by the *opsin3* gene in humans (Jiao et al. 2012) and may confer photosensitivity in extraocular tissues that are considered light-insensitive in vertebrates (Sugihara et al. 2018). The *opsin5* is a new type of short-wavelength sensitive photopigment in the brain of fish (Nakane et al. 2010) and as a photoreceptor, it can regulate seasonal changes in physiological behavior (Nakane et al. 2014). In *T. rubripes* larvae, *opsin3* and *opsin5* were expressed from 1 dah, implying that although vision seems to be the primary sense playing a key role in foraging activity and feeding, non-retinal photoreceptors such as the pineal organ and deep brain photoreceptors and non-visual opsins may be involved in fugu larval growth and development. Previous studies also have shown that the non-visual opsins *opsin3* and *opsin5* are expressed in inner retinal cells of chick retina at early phases of development and remain expressed in the mature retina at post-natal day 1 and 10 (Rios et al. 2019). Similarly, non-visual opsins including *opsin4a*, *tmtopsa*, *tmtopsb*, and *opsin3* are broadly expressed in the zebrafish larva central nervous system (Fernandes et al. 2013; Hang et al. 2016). *TMT -opsin*, *opsin4* and other non-visual opsins expression were detected in the telencephalon (rostral forebrain) of *Oryzias latipes* (Fischer et al. 2013). How these light-sensitive structures mediate photoperiodic signals and entrain key physiological events needs to be further clarified in fish.

In conclusion, the results obtained here suggest that the maturation of the eye of *T. rubripes* occurred during the transition period from endogenous to mixed feeding. The findings obtained here will provide implications for vision-based survival skills during the early life stages after hatching, and for the overall ecology and fitness of *T. rubripes*.

Declarations

Acknowledgments We are deeply grateful to other students from our research team, who were involved in the rearing process and sampling of specimens.

Authors' contributios Hongwei Yan conceived and designed the experiments; All the other authors contributed to material preparation, data collection and analysis. The original draf paper was written by Qi Zhang and all the other authors critically revised the manuscript.

Funding This research was supported by the grant of science and technology major project of Liaoning Province (2020JH1/10200002), the Youth Program of National Natural Science Foundation of China (31902347), the Projects for Dalian Youth Star of Science and Technology (2019RQ130), Liaoning Education Department Project (LJKZ0712), the Scientific, Technological and Innovation Program of Dalian (2021JJ11CG001)

Ethics approval All animal work was performed according to the Guide for the Care and Use of the Key Laboratory of Environment Controlled Aquaculture, Ministry of Education at Dalian Ocean University,

Dalian, China. All animal experiments complied with Chinese laws, regulations, and ethics, and were approved by Dalian Ocean University.

Consent to participate All the authors equally participated to prepare the manuscript in all stages.

Consent for publication All the authors approved to submit the present manuscript to Fish Physiology and Biochemistry.

Conflicts of interest The authors declare no competing interests.

Availability of data and material/ Data availability Not applicable

Code availability Not applicable

References

1. Aksnes DL, Giske J (1993) A theoretical model of aquatic visual feeding. Ecol Modell 67(2–4):233–250. https://doi.org/10.1016/0304-3800(93)90007-F
2. Ali MA, Anctil M (1977) Retinal structure and function in the walleye (*Stizostedion vitreum vitreum*) and sauger (*S. canadense*). J Fish Res Board Can 34(10):1467–1474. https://doi.org/10.1139/f77-211
3. Allen DM, Hallows TE (1997) Solar pruning of retinal rods in albino rainbow trout. Vis Neurosci 14(3):589–600. https://doi.org/10.1017/S0952523800012244
4. Álvarez-Hernán G, Andrade JP, Escarabajal-Blázquez L, Blasco M, Solana-Fajardo J, Martín-Partido G, Francisco-Morcillo J (2019) Retinal differentiation in syngnathids: comparison in the developmental rate and acquisition of retinal structures in altricial and precocial fish species. Zoomorphology 138(3):371–385. https://doi.org/10.1007/s00435-019-00447-3
5. Athanasiou D, Kosmaoglou M, Kanuga N, Novoselov SS, Paton AW, Paton JC et al (2012) BiP prevents rod opsin aggregation. Mol Biol Cell 23(18):3522–3531. https://doi.org/10.1091/mbc.e12-02-0168
6. Beaudry FEG, Iwanicki TW, Mariluz BRZ, Darnet S, Brinkmann H, Schneider P, Taylor JS (2017) The non-visual opsins: eighteen in the ancestor of vertebrates, astonishing increase in ray-finned fish, and loss in amniotes. J Exp Zool B Mol Dev Evol 328(7):685–696. https://doi.org/10.1002/jez.b.22773
7. Bejarano-Escobar R, Blasco M, Durán AC, Rodríguez C, Martín Partido G, Francisco-Morcillo J (2012) Retinal histogenesis and cell differentiation in an elasmobranch species, the small-spotted catshark *Scyliorhinus canicula*. J Anat 220(4):318–335. https://doi.org/10.1111/j.1469-7580.2012.01480.x
8. Bejarano-Escobar R, Blasco M, Durán AC, Martín-Partido G, Francisco-Morcillo J (2013) Chronotopographical distribution patterns of cell death and of lectin-positive macrophages/microglial cells during the visual system ontogeny of the small-spotted catshark *Scyliorhinus canicula*. J Anat 223(2):171–184. https://doi.org/10.1111/joa.12071

9. Bejarano-Escobar R, Blasco M, Martín-Partido G, Francisco-Morcillo J (2014) Molecular characterization of cell types in the developing, mature, and regenerating fish retina. Rev Fish Biol Fish 24(1):127–158. https://doi.org/10.1007/s11160-013-9320-z
10. Blaxter JHS, Staines ME (1971) Food searching potential in marine fish larvae. In Crisp DJ (ed) Fourth European marine biology symposium. Cambridge University Press, Cambridge, pp 467–485
11. Boeuf G, Le Bail PY (1999) Does light have an influence on fish growth? Aquaculture 177(1–4):129–152. https://doi.org/10.1016/S0044-8486(99)00074-5
12. Bonvini E, Parma L, Gatta PP, Mandrioli L, Sirri R, Martelli G, Nannoni E, Mordenti A, Bonaldo A (2016) Effects of light intensity on growth, feeding activity and development in common sole (*Solea solea* L.) larvae in relation to sensory organ ontogeny. Aquac Res 47:1809–1819. https://doi.org/10.1111/are.12639
13. Browman HI, Novales-Flamarique I, Hawryshyn CW (1994) Ultraviolet photoreception contributes to prey search behaviour in two species of zooplanktivorous fishes. J Exp Biol 186:187–198. https://doi.org/10.1242/jeb.186.1.187
14. Candal E, Anadón R, DeGrip WJ, Rodríguez-Moldes I (2005) Patterns of cell proliferation and cell death in the developing retina and optic tectum of the brown trout. Dev brain res 154(1):101–119. https://doi.org/10.1016/j.devbrainres.2004.10.008
15. Candal E, Ferreiro-Galve S, Anadón R, Rodríguez-Moldes I (2008) Morphogenesis in the retina of a slow-developing teleost: emergence of the GABAergic system in relation to cell proliferation and differentiation. Brain Res 1194:21–27. https://doi.org/10.1016/j.brainres.2007.11.065
16. Carleton KL, Spady TC, Streelman JT, Kidd MR, McFarland WN, Loew ER (2008) Visual sensitivities tuned by heterochronic shifts in opsin gene expression. BMC Biol 6(1):1–14. https://doi.org/10.1186/1741-7007-6-22
17. Caves EM, Brandley NC, Johnsen S (2018) Visual acuity and the evolution of signals. Trends Ecol Evol 33(5):358–372. https://doi.org/10.1016/j.tree.2018.03.001
18. Cehajic-Kapetanovic J, Eleftheriou C, Allen AE, Milosavljevic N, Pienaar A, Bedford R et al (2015) Restoration of vision with ectopic expression of human *rod opsin*. Curr Biol 25(16):2111–2122. https://doi.org/10.1016/j.cub.2015.07.029
19. Chi L, Li X, Liu Q, Liu Y (2017) Photoperiod regulate gonad development via kisspeptin/kissr in hypothalamus and saccus vasculosus of Atlantic salmon (*Salmo salar*). PLoS ONE 12:e0169569. https://doi.org/10.1371/journal.pone.0169569
20. Chinen A, Hamaoka T, Yamada Y, Kawamura S (2003) Gene duplication and spectral diversification of cone visual pigments of zebrafish. Genetics 163(2):663–675. https://doi.org/10.1093/genetics/163.2.663
21. Collin SP, Knight MA, Davies WL, Potter IC, Hunt DM, Trezise AE (2003) Ancient colour vision: multiple opsin genes in the ancestral vertebrates. Curr Biol 13(22):R864–R865. https://doi.org/10.1016/j.cub.2003.10.044

22. Cortesi F, Musilová Z, Stieb SM, Hart NS, Siebeck UE, Malmstrøm M et al (2015) Ancestral duplications and highly dynamic opsin gene evolution in percomorph fishes. Proc Natl Acad Sci USA 112(5):1493–1498. https://doi.org/10.1073/pnas.1417803112
23. De Miguel E, Anadón R (1987) The development of retina and the optic tectum of petromyzon marinus, L. A light microscopic study. J Hirnforsch 28(4):445–456
24. de Mera-Rodríguez JA, Álvarez-Hernán G, Gañán Y, Martín-Partido G, Rodríguez-León J, Francisco-Morcillo J (2019) Senescence-associated β-galactosidase activity in the developing avian retina. Dev Dyn 248(9):850–865. https://doi.org/10.1002/dvdy.74
25. Escobar-Camacho D, Ramos E, Martins C, Carleton KL (2017) The opsin genes of amazonian cichlids. Mol Ecol 26(5):1343–1356. https://doi.org/10.1111/mec.13957
26. Evans BI, Browman HI (2004) Variation in the development of the fish retina. Am Fish Soc Symp 40:145–166
27. Fernandes AM, Fero K, Driever W, Burgess HA (2013) Enlightening the brain: linking deep brain photoreception with behavior and physiology. BioEssays 35(9):775–779. https://doi.org/10.1002/bies.201300034
28. Fernald RD (1990) Teleost vision: seeing while growing. J Exp Zool 256(S5):167–180. https://doi.org/10.1002/jez.1402560521
29. Ferreiro-Galve S, Candal E, Carrera I, Anadón R, Rodríguez-Moldes I (2008) Early development of GABAergic cells of the retina in sharks: an immunohistochemical study with GABA and GAD antibodies. J Chem Neuroanat 36(1):6–16. https://doi.org/10.1016/j.jchemneu.2008.04.004
30. Ferreiro-Galve S, Rodríguez-Moldes I, Anadón R, Candal E (2010a) Patterns of cell proliferation and rod photoreceptor differentiation in shark retinas. J Chem Neuroanat 39(1):1–14. https://doi.org/10.1016/j.jchemneu.2009.10.001
31. Ferreiro-Galve S, Rodríguez-Moldes I, Candal E (2010b) Calretinin immunoreactivity in the developing retina of sharks: comparison with cell proliferation and GABAergic system markers. Exp Eye Res 91(3):378–386. https://doi.org/10.1016/j.exer.2010.06.011
32. Ferreiro-Galve S, Rodríguez-Moldes I, Candal E (2012) Pax6 expression during retinogenesis in sharks: comparison with markers of cell proliferation and neuronal differentiation. J Exp Zool B Mol Dev Evol 318(2):91–108. https://doi.org/10.1002/jezb.21448
33. Fischer RM, Fontinha BM, Kirchmaier S, Steger J, Bloch S, Inoue D, Tessmar-Raible K (2013) Co-expression of VAL-and TMT-opsins uncovers ancient photosensory interneurons and motorneurons in the vertebrate brain. PLOS Biol 11(6):e1001585. https://doi.org/10.1371/journal.pbio.1001585
34. Flamarique IN, Hawryshyn CW (1996) Retinal development and visual sensitivity of young Pacific sockeye salmon (*Oncorhynchus nerka*). J Exp Biol 199(4):869–882. https://doi.org/10.1242/jeb.199.4.869
35. Gao XQ, Hong L, Liu ZF, Guo ZL, Wang YH, Lei JJ (2016) Histological Observation of the Eye of American Shad (*Alosa sapidissima*) at the Early Developmental Stage. Progress In Fishery Science 37(2):76–83. https://doi.org/10.11758/yykxjz.20150104002

36. García-López Á, Pascual E, Sarasquete C, Martínez-Rodríguez G (2006) Disruption of gonadal maturation in cultured Senegalese sole *Solea senegalensis* Kaup by continuous light and/or constant temperature regimes. Aquaculture 261:789–798. https://doi.org/10.1016/j.aquaculture.2006.09.005
37. Guido ME, Marchese NA, Rios MN, Morera LP, Diaz NM, Garbarino-Pico E, Contin MA (2020) Non-visual opsins and novel photo-detectors in the vertebrate inner retina mediate light responses within the blue spectrum region. Cell Mol Neurobiol 1–25. https://doi.org/10.1007/s10571-020-00997-x
38. Guthrie DM, Muntz WRA (1993) The role of vision in fish behaviour.. In: In: Pitcher TJ (ed) Behavior of Teleost Fishes, 2nd edn. Chapman, London, pp 89–128
39. Hang CY, Kitahashi T, Parhar IS (2016) Neuronal organization of deep brain opsin photoreceptors in adult teleosts. Front Neurosci 10:48. https://doi.org/10.3389/fnana.2016.00048
40. Harahush BK, Hart NS, Green K, Collin SP (2009) Retinal neurogenesis and ontogenetic changes in the visual system of the brown banded bamboo shark, *Chiloscyllium punctatum* (Hemiscyllidae, Elasmobranchii). J Comp Neurol 513(1):83–97. https://doi.org/10.1002/cne.21953
41. Hargrave PA, McDowell JH, Curtis DR, Wang JK, Juszczak E, Fong SL et al (1983) The structure of bovine rhodopsin. Biophys Struct Mech 9(4):235–244. https://doi.org/10.1007/BF00535659
42. He DR, Zhou SJ, Liu LD, Cai HC, Zhen WY (1985) A study on the optomotor reaction of some young fishes. Acta Hydrobiol Sin 9(4):365–373
43. Hu J, Liu Y, Ma Z, Qin JG (2018) Feeding and development of warm water marine fish larvae in early life.. In: In: Manuel Y (ed) Emerging Issues in Fish Larvae Research. Springer, New York, pp 275–296. https://doi.org/10.1007/978-3-319-73244-2_10
44. Jacobs GH, Neitz M, Neitz J (1996) Mutations in S-cone pigment genes and the absence of colour vision in two species of nocturnal primate. Proc Biol Sci 263(1371):705–710. https://doi.org/10.1098/rspb.1996.0105
45. Jenkins A, Muñoz M, Tarttelin EE, Bellingham J, Foster RG, Hankins MW (2003) VA opsin, melanopsin, and an inherent light response within retinal interneurons. Curr Biol 13(15):1269–1278. https://doi.org/10.1016/S0960-9822(03)00509-8
46. Jiao J, Hong S, Zhang J, Ma L, Sun Y, Zhang D et al (2012) Opsin3 sensitizes hepatocellular carcinoma cells to 5-fluorouracil treatment by regulating the apoptotic pathway. Cancer Lett 320(1):96–103. https://doi.org/10.1016/j.canlet.2012.01.035
47. Jones MR, Grillner S, Robertson B (2009) Selective projection patterns from subtypes of retinal ganglion cells to tectum and pretectum: distribution and relation to behavior. J Comp Neurol 517(3):257–275. https://doi.org/10.1002/cne.22154
48. Kasagi S, Mizusawa K, Murakami N, Andoh T, Furufuji S, Kawamura S, Takahashi A (2015) Molecular and functional characterization of opsins in barfin flounder (*Verasper moseri*). Gene 556(2):182–191. https://doi.org/10.1016/j.gene.2014.11.054
49. Katamachi D, Ikeda M, Uno K (2015) Identification of spawning sites of the tiger puffer *Takifugu rubripes* in Nanao Bay, Japan, using DNA analysis. Fish Sci 81(3): 485–494.

https://doi.org/10.1007/s12562-015-0867-6

50. Kim BJ, Choi SH, Kim S (2013) Description of a small goby, *Trimma grammistes* (Perciformes: Gobiidae), from Jeju Island. Korea Ocean Sci J 48(2):235–238. https://doi.org/10.1007/s12601-013-0020-3
51. Kim BH, Hur SP, Hur SW, Lee CH, Lee YD (2016) Relevance of light spectra to growth of the rearing tiger puffer *Takifugu rubripes*. Dev Rerprod 20:23–29. https://doi.org/10.12717/DR.2016.20.1.023
52. Kim ES, Lee CH, Lee YD (2019) Retinal development and opsin gene expression during the juvenile development in red spotted grouper *(Epinephelus akaara*). Dev Rerprod 23(2):171. https://doi.org/10.12717/DR.2019.23.2.171
53. Kimmel CB, Ballard WW, Kimmel SR, Ullmann B, Schilling TF (1995) Stages of embryonic development of the zebrafish. Dev Dyn 203(3):253–310. https://doi.org/10.1002/aja.1002030302
54. Kolb H (2011) Simple anatomy of the retina by helga kolb. Webvision: The Organization of the Retina and Visual System. http://webvision.med.utah.edu/book/part-i-foundations/simple-anatomy-of-the-retina
55. Kusmic C, Gualtieri P (2000) Morphology and spectral sensitivities of retinal and extraretinal photoreceptors in freshwater teleosts. Micron 31(2):183–200. https://doi.org/10.1016/S0968-4328(99)00081-5
56. Li F, Guo ZD, Liu BX, Wang ZJ (2016) Early eye morphogenesis in the chinese sucker (*myxocyprinus asiaticus*). Acta Hydrobiol Sin 40(3):7. https://doi.org/10.7541/2016.68
57. Lim LS, Mukai Y (2014) Morphogenesis of sense organs and behavioural changes in larvae of the brown-marbled grouper *Epinephelus fuscoguttatus* (Forsskål). Mar Freshw Behav Physiol 47(5):313–327. https://doi.org/10.1080/10236244.2014.940689
58. Liu Q, Yan H, Hu P, Liu W, Shen X, Cui X et al (2019) Growth and survival of *Takifugu rubripes* larvae cultured under different light conditions. Fish Physiol Biochem 45(5):1533–1549. https://doi.org/10.1007/s10695-019-00639-0
59. Loew ER, McFarland WN, Mills EL, Hunter D (1993) A chromatic action spectrum for planktonic predation by juvenile yellow perch, *Perca flavescens*. Can J Zool 71:384–386. https://doi.org/10.1139/z93-053
60. Ma AJ, Wang XA, Zhuang ZM, Zhang XM (2010) Structure of retina and visual characteristics of the half-smooth tongue-sole *Cynoglossus semilaevis Günter*. Acta Zoologica Sinica 2010: 354–363
61. Mader MM, Cameron DA (2004) Photoreceptor differentiation during retinal development, growth, and regeneration in a metamorphic vertebrate. J Neurosci 24(50):11463–11472. https://doi.org/10.1523/JNEUROSCI.3343-04.2004
62. Matsumoto Y, Fukamachi S, Mitani H, Kawamura S (2006) Functional characterization of visual opsin repertoire in Medaka (*Oryzias latipes*). Gene 371(2):268–278. https://doi.org/10.1016/j.gene.2005.12.005
63. Miranda V, Cohen S, Díaz AO, Diaz MV (2020) Development of the visual system of anchovy larvae, *Engraulis anchoita*: A microanatomical description. J Morphol 281(4–5):465–475.

https://doi.org/10.1002/jmor.21113

64. Munz FW, McFarland WN (1973) The significance of spectral position in the rhodopsins of tropical marine fishes. Vision Res 13(10):1829–1IN1. https://doi.org/10.1016/0042-6989(73)90060-6
65. Musilova Z, Cortesi F, Matschiner M, Davies WI, Patel JS, Stieb SM et al (2019) Vision using multiple distinct rod opsins in deep-sea fishes. Science 364(6440):588–592. https://doi.org/10.1126/science.aav4632
66. Nakane Y, Ikegami K, Ono H, Yamamoto N, Yoshida S, Hirunagi K et al (2010) A mammalian neural tissue opsin (*Opsin 5*) is a deep brain photoreceptor in birds. Proc Natl Acad Sci USA 107(34):15264–15268. https://doi.org/10.1073/pnas.1006393107
67. Nakane Y, Shimmura T, Abe H, Yoshimura T (2014) Intrinsic photosensitivity of a deep brain photoreceptor. Curr Biol 24(13):R596–R597. https://doi.org/10.1016/j.cub.2014.05.038
68. Neafsey DE, Hartl DL (2005) Convergent loss of an anciently duplicated, functionally divergent RH2 opsin gene in the fugu and Tetraodon pufferfish lineages. Gene 350(2):161–171. https://doi.org/10.1016/j.gene.2005.02.011
69. Novelli B, Socorro JA, Caballero MJ, Otero-Ferrer F, Segade BA, Domínguez LM (2015) Development of seahorse (*Hippocampus reidi*, Ginsburg 1933): histological and histochemical study. Fish Physiol Biochem 41(5):1233–1251. https://doi.org/10.1007/s10695-015-0082-5
70. Palczewski K, Kumasaka T, Hori T, Behnke CA, Motoshima H, Fox BA et al (2000) Crystal structure of rhodopsin: AG protein-coupled receptor. Science 289(5480):739–745. https://doi.org/10.1126/science.289.5480.739
71. Parry JW, Carleton KL, Spady T, Carboo A, Hunt DM, Bowmaker JK (2005) Mix and match color vision: tuning spectral sensitivity by differential opsin gene expression in Lake Malawi cichlids. Curr Biol 15(19):1734–1739. https://doi.org/10.1016/j.cub.2005.08.010
72. Pavón-Muñoz T, Bejarano-Escobar R, Blasco M, Martín-Partido G, Francisco-Morcillo J (2016) Retinal development in the gilthead seabream *Sparus aurata*. J Fish Biol 88(2):492–507. https://doi.org/10.1111/jfb.12802
73. Prasad S, Galetta SL (2011) Anatomy and physiology of the afferent visual system. Handb Clin Neurol 102:3–19. https://doi.org/10.1016/B978-0-444-52903-9.00007-8
74. Reckel F, Melzer RR, Parry JWL, Bowmaker JK (2002) The retina of five atherinomorph teleosts: photoreceptors, patterns and spectral sensitivities. Brain Behav Evol 60(5):249–264. https://doi.org/10.1159/000067191
75. Rennison DJ, Owens GL, Taylor JS (2012) Opsin gene duplication and divergence in ray-finned fish. Mol Phylogenet Evol 62(3):986–1008. https://doi.org/10.1016/j.ympev.2011.11.030
76. Rios MN, Marchese NA, Guido ME (2019) Expression of non-visual opsins Opn3 and Opn5 in the developing inner retinal cells of birds. Light-responses in Müller glial cells. Front Cell Neurosci 13:376. https://doi.org/10.3389/fncel.2019.00376
77. Rodicio MC, Pombal MA, Anadón R (1995) Early development and organization of the retinopetal system in the larval sea lamprey. Petromyzon marinus L Anat Embryol 192(6):517–526.

https://doi.org/10.1007/BF00187182

78. Rønnestad I, Yúfera M, Ueberschär B, Ribeiro L, Sæle Ø, Boglione C (2013) Feeding behaviour and digestive physiology in larval fish: current knowledge, and gaps and bottlenecks in research. Rev Aquac 5:S59–S98. https://doi.org/10.1111/raq.12010
79. Rubinson K (1990) The developing visual system and metamorphosis in the lamprey. J Neurosci 21(7):1123–1135. https://doi.org/10.1002/neu.480210715
80. Sánchez-Farías N, Candal E (2015) Doublecortin is widely expressed in the developing and adult retina of sharks. Exp Eye Res 134:90–100. https://doi.org/10.1016/j.exer.2015.04.002
81. Sánchez-Farías N, Candal E (2016) Identifcation of radial glia progenitors in the developing and adult retina of sharks. Front Neuroanat 10:65. https://doi.org/10.3389/fnana.2016.00065
82. Sandy JM, Blaxter JHS (1980) A study of retinal development in larval herring and sole. J Mar Biolog Assoc UK 60(1):59–71. https://doi.org/10.1017/S0025315400024115
83. Sanyal S, Zeilmaker GH (1988) Retinal damage by constant light in chimaeric mice: implications for the protective role of melanin. Exp Eye Res 46(5):731–743. https://doi.org/10.1016/S0014-4835(88)80059-9
84. Schieber NL, Collin SP, Hart NS (2012) Comparative retinal anatomy in four species of elasmobranch. J Morphol 273(4):423–440. https://doi.org/10.1002/jmor.11033
85. Shichida Y, Imai H (1998) Visual pigment: G-protein-coupled receptor for light signals. Cell Mol Life Sci 54(12):1299–1315. https://doi.org/10.1007/s000180050256
86. Spady TC, Parry JW, Robinson PR, Hunt DM, Bowmaker JK, Carleton KL (2006) Evolution of the cichlid visual palette through ontogenetic subfunctionalization of the opsin gene arrays. Mol Biol Evol 23(8):1538–1547. https://doi.org/10.1093/molbev/msl014
87. Stuart KR (2013) The effect of light on larval rearing in marine finfish.. In: In: Qin JG (ed) Larval fish aquaculture. Nova Science Publisher Inc, New York, pp 25–40
88. Sugihara T (2018) Investigation of molecular properties of vertebrate non-visual opsin, Opn3 (Dissertation, Osaka City University)
89. Terakita A (2005) The opsins. Genome Biol 6(3):1–9. https://doi.org/10.1186/gb-2005-6-3-213
90. Van Hazel I, Santini F, Müller J, Chang BS (2006) Short-wavelength sensitive opsin (*SWS1*) as a new marker for vertebrate phylogenetics. BMC Evol Biol 6(1):1–15. https://doi.org/10.1186/1471-2148-6-97
91. Villeneuve LA, Gisbert E, Moriceau J, Cahu CL, Infante JLZ (2006) Intake of high levels of vitamin A and polyunsaturated fatty acids during different developmental periods modifies the expression of morphogenesis genes in European sea bass (*Dicentrarchus labrax*). Br J Nutr 95(4):677–687. https://doi.org/10.1079/BJN20051668
92. Watson CT, Gray SM, Hoffmann M, Lubieniecki KP, Joy JB, Sandkam BA et al (2011) Gene duplication and divergence of long wavelength-sensitive opsin genes in the guppy, *Poecilia reticulata*. J Mol Evol 72(2):240–252. https://doi.org/10.1007/s00239-010-9426-z

93. Xu YG, He DR (1988) Preliminary study on the retinomotor responses of juvenile *sparus latus* and *mugil cephalus*.Oceanologia Et Limnologia Sinica(02):109–115
94. Yokoyama S (1997) Molecular genetic basis of adaptive selection: examples from color vision in vertebrates. Annu Rev Genet 31(1):315–336. https://doi.org/10.1146/annurev.genet.31.1.315
95. Yokoyama S (2000) Molecular evolution of vertebrate visual pigments. Prog Retin Eye Res 19(4):385–419. https://doi.org/10.1016/S1350-9462(00)00002-1
96. Yúfera M, Ortiz-Delgado JB, Hoffman T, Siguero I, Urup B, Sarasquete C (2014) Organogenesis of digestive system, visual system and other structures in Atlantic bluefin tuna (*Thunnus thynnus*) larvae reared with copepods in mesocosm system. Aquaculture 426:126–137. https://doi.org/10.1016/j.aquaculture.2014.01.031
97. Zhang N, Wang W, Li B, Liu Y (2019) Non-volatile taste active compounds and umami evaluation in two aquacultured pufferfish (*Takifugu obscurus* and *Takifugu rubripes*). Food Biosci 32:100468. https://doi.org/10.1016/j.fbio.2019.100468
98. Zhang N, Wang W, Li B, Liu Y (2019) Non-volatile taste active compounds and umami evaluation in two aquacultured pufferfish (*Takifugu obscurus* and *Takifugu rubripes*). Food Biosci 32: 100468. https://doi.org/10.1016/j.fbio.2019.100468

Figures

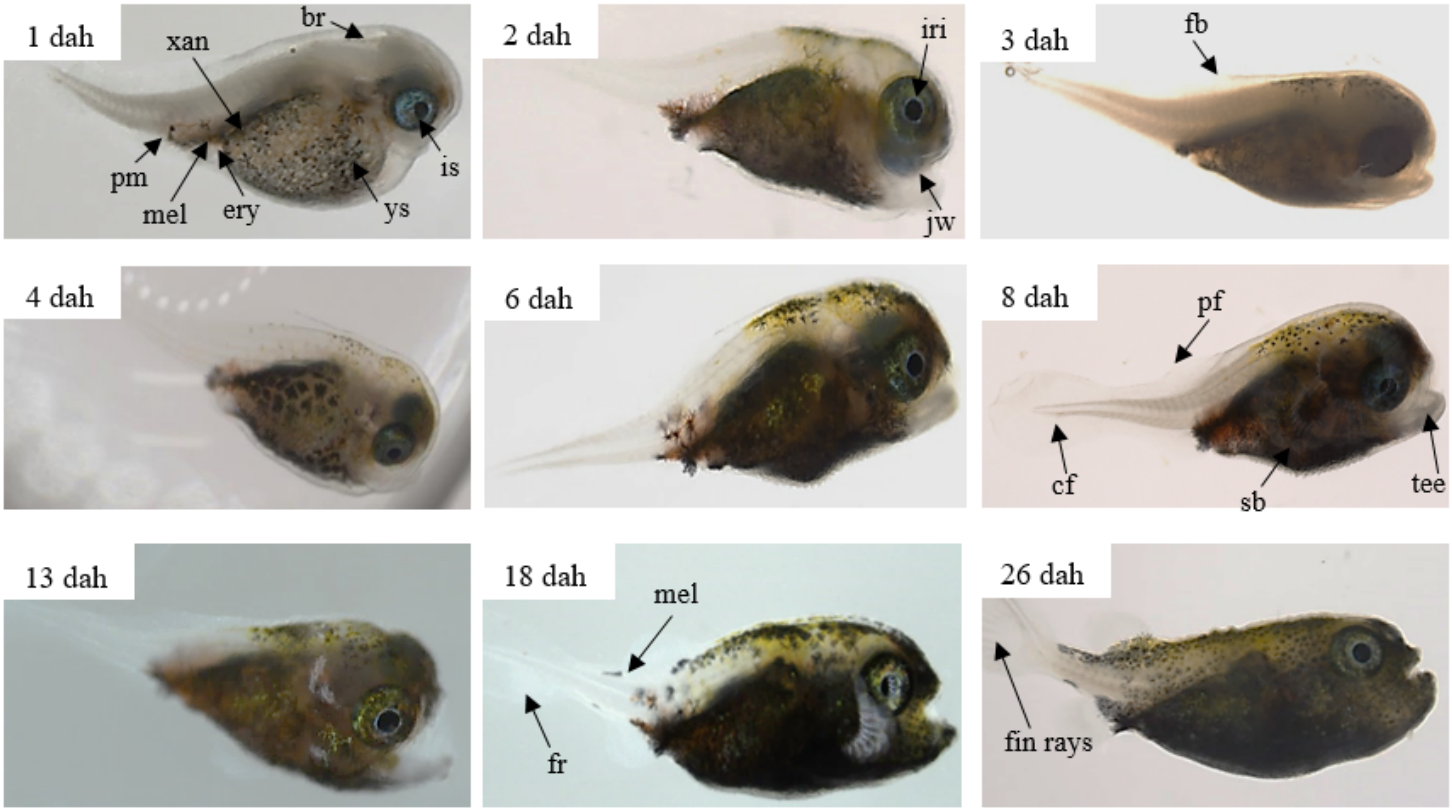

Figure 1

Photographs of *Takifugu rubripes* during different sampling points. dah, days after hatching. br, brain; cf, caudal fin; ery, erythrophores; fb, fin buds; fr, filamentous rays; iri, iridiophores; is, iris; jw, jaws; mel, melanophores; pf, pectoral fin; pm, pigment margin; sb, swim bladder; tee, teeth; xan, xanthophore; ys, yolk sac.

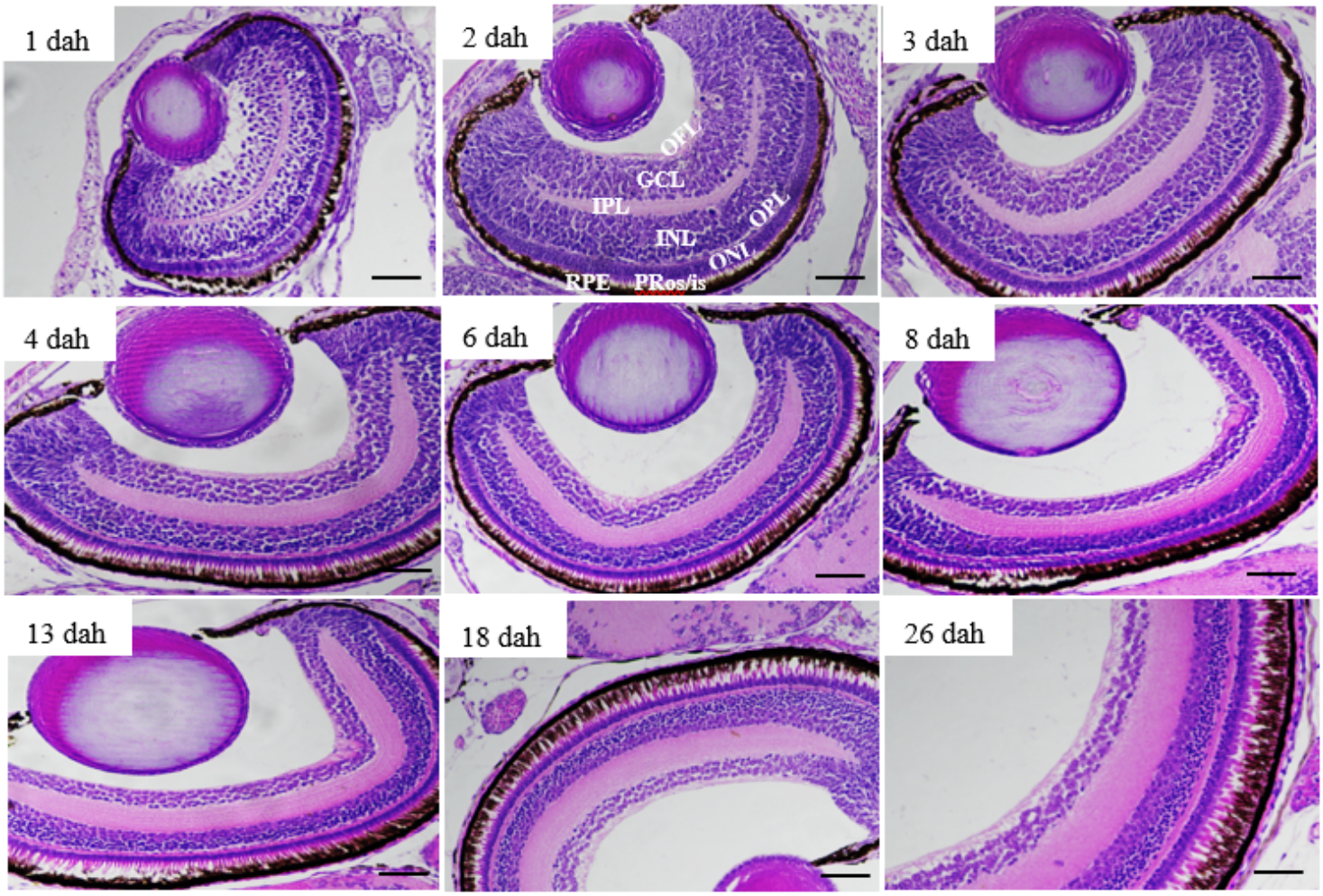

Figure 2

Histological sections of retina of *T. rubripes* larvae at different developmental stages. RPE, retinal pigment epithelium layer; PRos/is, photoreceptor layer (including RPE, PRos, and PRis); ONL, outer nuclear layer; OPL, outer plexiform layer; INL, inner nuclear layer; IPL, inner plexiform layer; GCL, ganglion cell layer; OFL, optic fiber layer. Scale bar = 50 μm

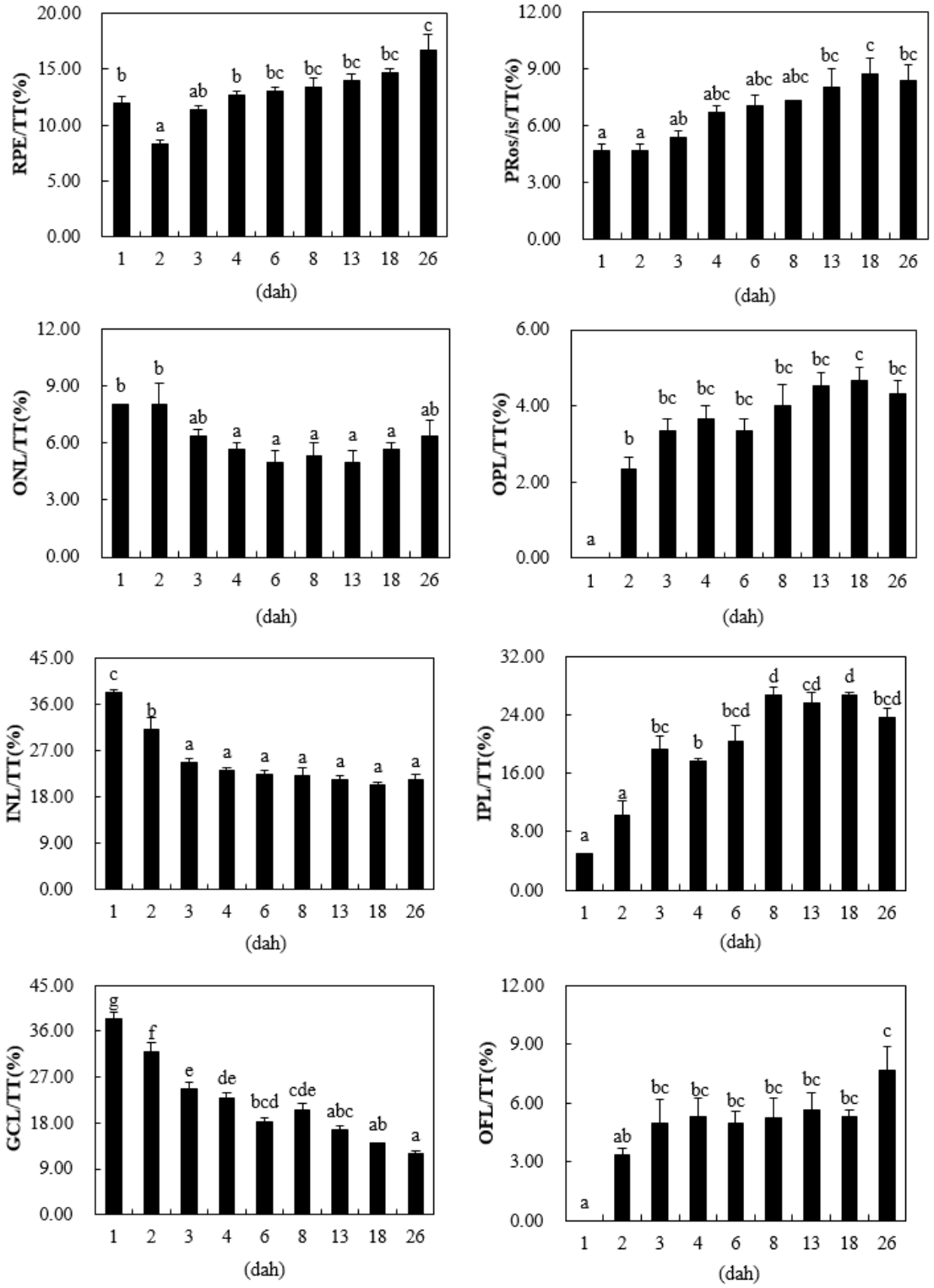

Figure 3

The ratio of the thickness of each layer to the total thickness of the retina of *T. rubripes* larvae at different developmental stages. Data are expressed as the means ± SEM (n=9). Different lowercase letters indicate statistically significant differences between each treatment (one-way ANOVA, $P<0.05$, n=3)

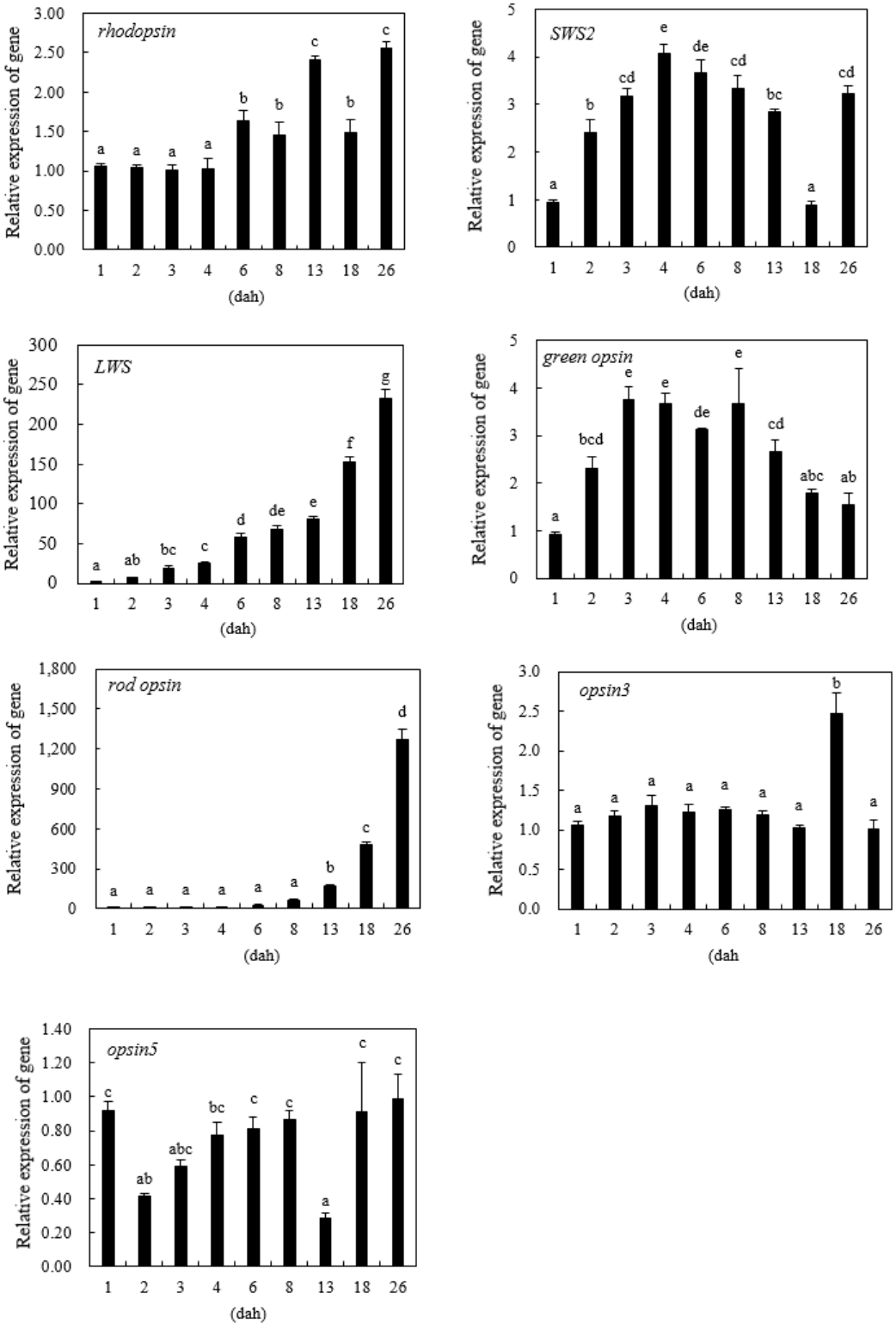

Figure 4

The relative mRNA expression levels of *green opsin*, *SWS2*, *LWS*, *rod opsin*, *rhodopsin*, *opsin3* and *opsin5* in *T. rubripes* at different developmental stages. Data are expressed as the means ± SEM (n=9). Different lowercase letters indicate statistically significant differences between each treatment (one-way ANOVA, $P<0.05$, n=3)